J Nanostruct 12(3): 746-753, Summer 2022

RESEARCH PAPER

# Mn/Cu/O/ Chitosan Nanocomposites: Hydrothermal Synthesis, Characterization, and Its Application for Adsorptive Removal of Methylene Blue from Wastewater

*Azam Sobhani*

*Department of Chemistry, Kosar University of Bojnord, Bojnord, Islamic Republic of Iran*

ARTICLE INFO

***Article History:***
*Received 15 April 2022*
*Accepted 27 June 2022*
*Published 01 July 2022*

***Keywords:***
*Adsorption*
*Chitosan*
*Hydrothermal*
*Metal oxide*
*Nanocomposite*

ABSTRACT

In this study, a green process for the synthesis of Mn and Cu oxides in chitosan membranes is reported. The process consists of two steps: (1) synthesis of $Mn/Mn_2O_3$ nano/microstructures in the presence of onion via hydrothermal method, (2) synthesis of Mn/Cu/O/chitosan nanocomposites using chitosan, CuO powder, and $Mn/Mn_2O_3$ prepared in the first step. The SEM images showed formation of the bundles of spherical Mn/Cu/O/chitosan nanocomposites. The XRD patterns confirmed the formation of the nanocomposites. The problem of water pollution is of a great concern and adsorption is one of the most efficient techniques for removing the pollution from the solvent phase. The nanocomposites synthesized in this work can help us to solve the waste disposal problem. They are effective adsorbents for MB and phenol removal from aqueous solution. In UV-Vis spectra, the intensity of peaks of MB and phenol are decreased after their adsorption on the surface of the nanocomposite.

**How to cite this article**
*Sobhani A. Mn/Cu/O/ Chitosan Nanocomposites: Hydrothermal Synthesis, Characterization, and Its Application for Adsorptive Removal of Methylene Blue from Wastewater. J Nanostruct, 2022; 12(3):746-753. DOI: 10.22052/JNS.2022.03.027*

## INTRODUCTION

Hydrothermal is a method for the crystal growth and synthesis of the nanostructures in an autoclave, under high pressure and in hot water [1–5]. This method is suitable for the growth of large good-quality crystals while maintaining control over their composition. Advantages of the hydrothermal method include the ability to create crystalline phases which are not stable at the melting point. Also, materials which have a high vapor pressure near their melting points can be grown by the hydrothermal method. We have selected this method because it is a simple method. The solvent used in this method is water as a cheap, abundant, green and interminable solvent.

Chitosan is a family of molecules with differences in their size, composition, and monomer distribution. It has garnered much interest due to its technological and biological performance, properties and applications [6]. In this work, we use the chitosan for the green synthesis of Mn/Cu/O/chitosan nanocomposites. The as-prepared nanocomposites help us to remove MB from the aqueous solution. MB is a cationic dye, biologically dangerous and control of its content is necessary [7]. Increased heart rate, quadriplegia, cyanosis, jaundice, shock, Heinz body formation, vomiting, and tissue necrosis are unfavorable effects on human health caused by MB [8]. Elimination of dye

* *Corresponding Author Email: sobhani@kub.ac.ir*

pollution from the solvent phase by adsorption is a necessary aspect of research [9–12]. The adsorption is considered as an efficient and low-cost technique for removing contaminants from water. Adsorption is the process taking place when a liquid solute (adsorbate) accumulates on the surface of an adsorbent. Adsorption is often accompanied by the inverse process for desorption, which represents the transfer of adsorbate ions from the adsorbent surface to the solution. Depending on the adsorbate amount desorbed from the adsorbent, one can judge the reversibility of adsorption [13]. There are two types of adsorption, including physical and chemical adsorptions. In physical adsorption, an increase in the adsorbate concentration at the interface is due to van der Waals forces, and chemisorption is caused by chemical reactions between the adsorbate and the adsorbent which create covalent or ionic bonds. Physical adsorption is weakly specific, reversible, its thermal effect is small, usually irreversible, its heat ranges from tens to hundreds of kJ/mol [14–16].

## MATERIALS AND METHODS

All the materials used in this work, including $Mn(NO_3)_2.4H_2O$, chitosan, and CuO were purchased from Merck company. An X-ray diffractometer (XRD) with Ni-filtered Cu Kα radiation and λ = 1.54 Å, Philips X'pertPro, was used to study structure and phase of the products. The morphology of the products was studied by a field emission scanning electron microscope (SEM), TESCAN Mira3 FE-SEM. UV–Vis spectra were taken by Evolution 300 spectrophotometer made in the American Thermo scientific company.

### *Synthesis of $Mn/Mn_2O_3$ nanostructures*

An aqueous solution of $Mn(NO_3)_2.4H_2O$ was prepared. Then 70 ml onion was added drop-wise into the solution under stirring. After stirring for 15 min, the final solution was transferred into a stainless steel Teflon-lined autoclave. The autoclave was sealed and maintained at 180 ˚C for 12 h. The autoclave was cooled to room temperature on its own with the rate of 1 ˚C/min. Then the products were washed with distilled water and anhydrous ethanol several times and calcined under vacuum at 400 ˚C for 2 h.

### *Synthesis of Mn/Cu/O/chitosan nanocomposites*

To prepare the Mn/Cu/O/chitosan nanocomposites, chitosan was dissolved in distilled water and acetic acid. Then CuO powder was dispersed in distilled water and added into the chitosan solution under strong magnetic stirring. In the next step, $Mn/Mn_2O_3$ nanostructures prepared in the before step were added. The weight ratio of Cu/Mn/chitosan used was 1:1:1. The mixture was stirred for 24 h until the water was vapored. The nanocomposites were washed with distilled water and ethanol several times, and dried under vacuum at 60 ˚C for 4 h.

### *Photocatalytic measurements*

In this work, the photocatalytic activity of Mn/Cu/O/chitosan nanocomposite was investigate. The methylene blue (MB) was used as contaminant dye. Eq. (1) estimates the photodegradation efficiency of MB:

$$\text{Degradation \%} = [(A_0 - A)/A_0] \times 100 \quad (1)$$

In this equation, A and $A_0$ are absorbance quantities of organic solution after and before decomposition, respectively [17].

## RESULTS AND DISCUSSION

The structural analysis of nanostructures and nanocomposites was investigated. XRD patterns of samples 1, 2 and 3 and also pure chitosan have been shown in Fig. 1. As shown in Fig. 1a, the product obtained in the presence of 70 ml onion via hydrothermal reaction of Mn salt (sample 1) is amorphous. XRD pattern of this sample after its calcination under vacuum at 400 ˚C for 2 h (sample 2), has been shown in Fig. 1b, it is a mixture of Mn and $Mn_2O_3$. Fig. 1c shows XRD pattern of pure chitosan with a sharp peak at 2Theta~20. Also, the XRD pattern of Mn/Cu/O/chitosan nanocomposite has been shown in Fig.1d. By comparing XRD patterns of this figure with Fig. 1c, it can be found that the peaks of the chitosan are weak in the XRD pattern of the nanocomposites. Other diffraction peaks in Fig. 1d related to Cu and Mn oxides. Also the intensity of these peaks is lower than those in Fig. 1b. The XRD patterns of the nano/microstructures (Fig. 1b) and nanocomposites (Fig. 1d) synthesized in this work are broad and low intensity, which suggest a low crystallinity and an amorphous nature of the products and or the formation of the products with small particle sizes. The weak peaks in Fig. 1d reflect great disarray in chain alignment of chitosan with the production

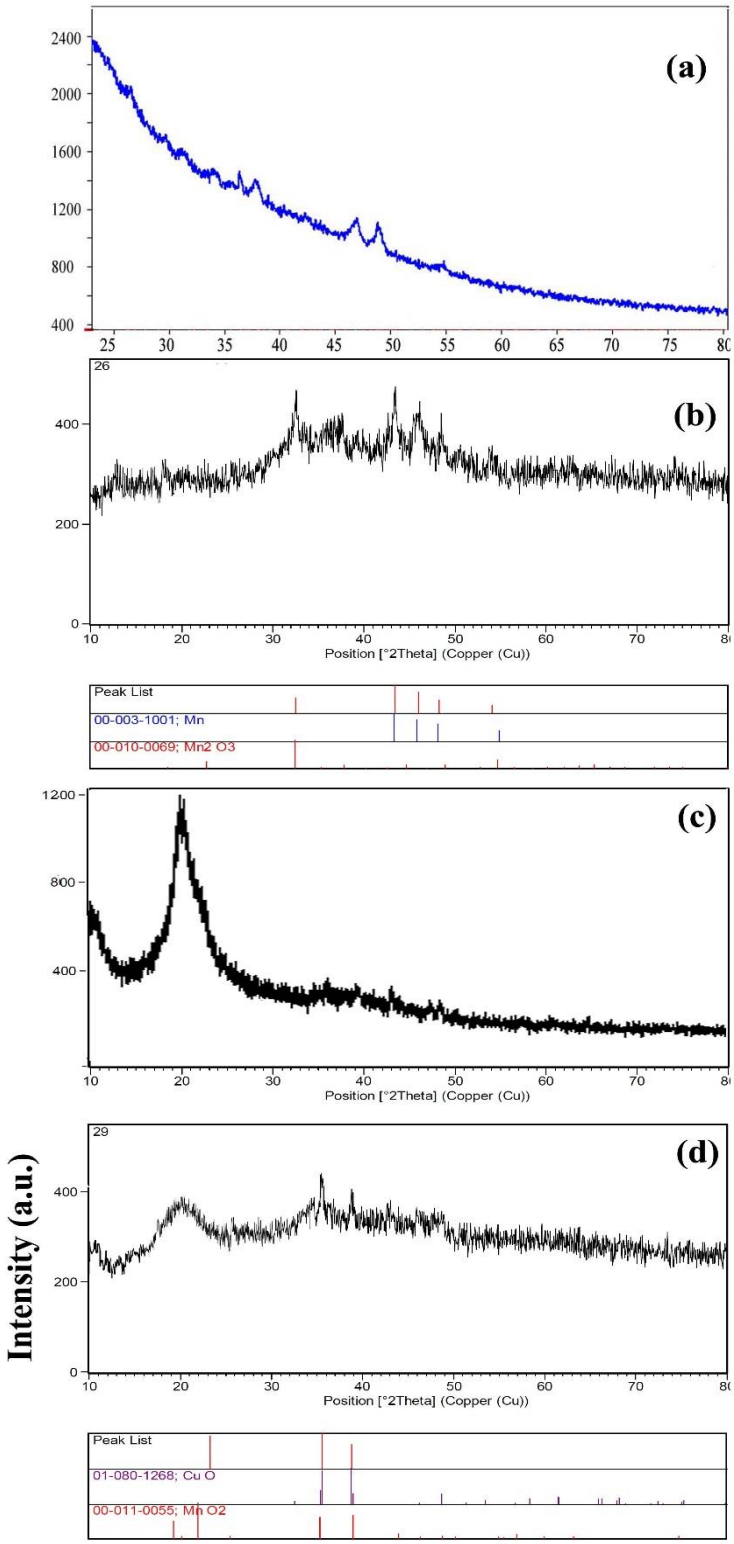


Fig. 1. XRD patterns of: (a) the product prepared in the presence of 70 ml onion via hydrothermal method of Mn sal (sample 1) , (b) the product prepared after calcination of sample 1 under vacuum at 400 ˚C (sample 2) , (c) Chitosan , (d) the nanocomposite prepared with chitosan (sample 3).

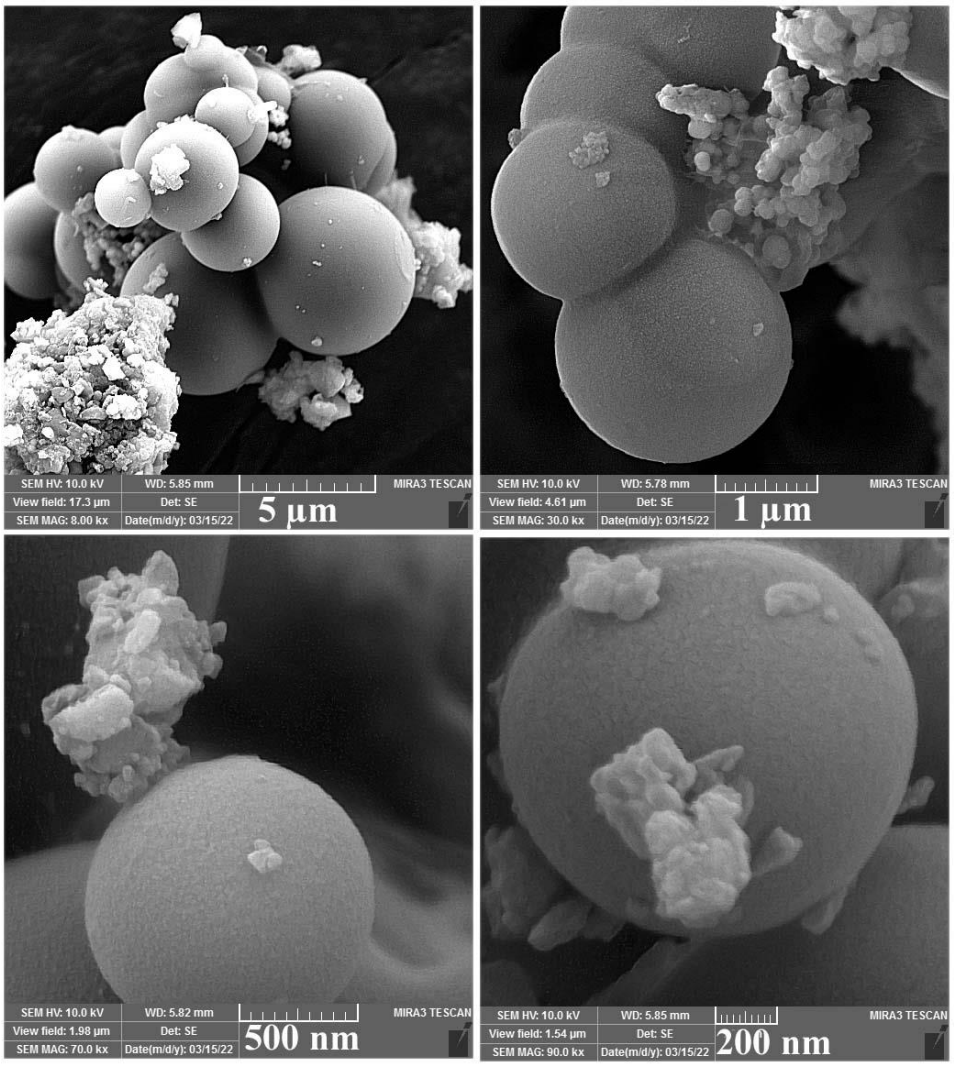


Fig. 2. SEM images of the nanocomposite prepared with chitosan (sample 3).

of new peaks that identify the presence of Cu and Mn oxides. These patterns reveal the successful inclusion of Cu and Mn oxides in nanocomposite membranes. Moreover, the presence of these metal oxides impede the order of polymer chains by both steric effect and intermolecular hydrogen bonds. So, the introduction of Cu and Mn oxides in chitosan decrease the crystallinity of composite membranes and increase the flexibility of polymer chain [18].

Fig. 2 shows SEM images of the nanocomposite prepared with chitosan (sample 3). The figure shows formation of the agglomerated spheres with diameters ranging from 1.5 µm to 7 µm. A closer look at this figure also shows the formation of the agglomerated nanoparticles on the spheres. The particle size distribution of the nanoparticles and microspheres is not uniform.

The UV-Vis absorbance spectra of the pure MB and MB adsorbed on the surface of Mn/Cu/O/ chitosan NC have been shown in Fig. 3a. The results confirm the application of as-prepared nanocomposites as an effective adsorbent for MB removal from aqueous solution. Also, Fig. 3b shows that these nanocomposites are effective adsorbents for phenol removal. In UV-Vis spectra in Fig. 3 show that the intensity of peaks of MB and phenol have been decreased after their adsorption on the surface of the nanocomposite.

In this work, the photocatalytic activity of the nanocomposites for the degradation of MB was investigated under visible and UV irradiations. Fig.

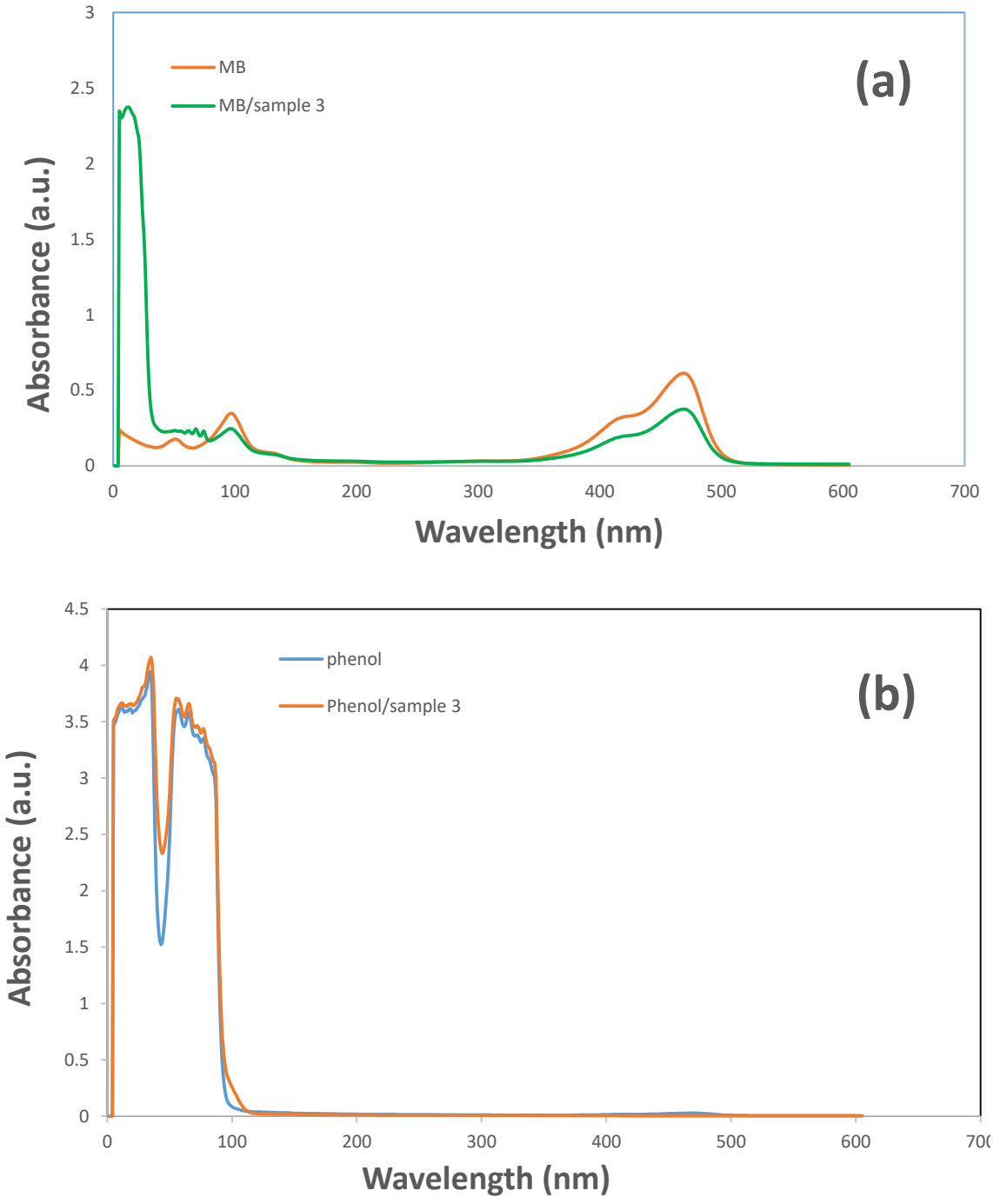


Fig. 3. Absorption spectra of: (a) MB and the solution obtained from centrifugation of MB/sample 3 suspension; (b) phenol and the solution obtained from centrifugation of the phenol/sample 3 suspension.

4 shows MB degradation under visible irradiation is higher than UV irradiation. This figure shows degradation percentage of MB in the presence of the Mn/Cu/O/chitosan NC is about 76 %, after 45 min visible light irradiation, while it is about 13% and 17.5 % after 45 and 60 min UV light irradiation, respectively. Thus the as-prepared nanocomposites in this work can be used as an

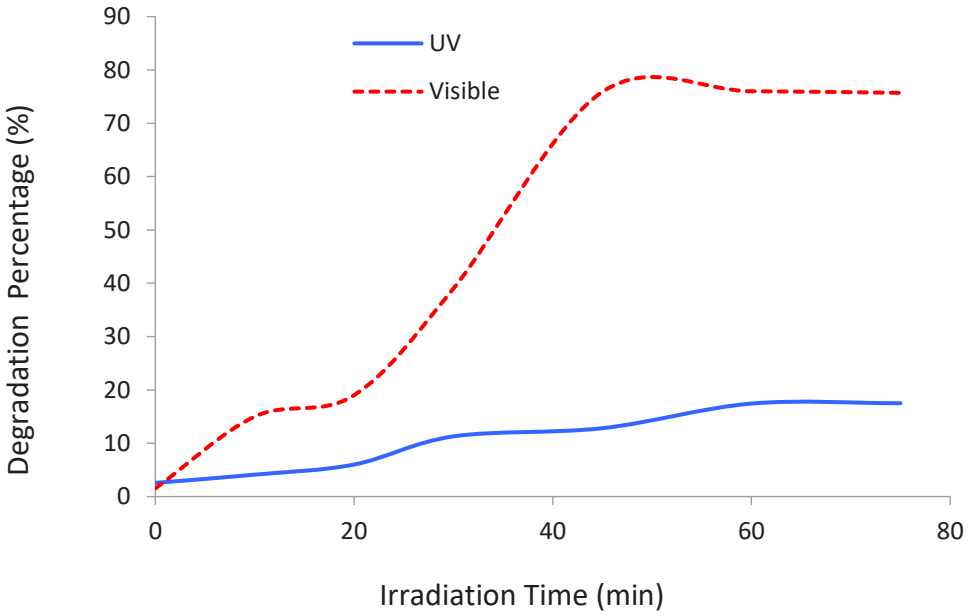


Fig. 4. Photocatalytic activity of the nanocomposites for degradation of MB under visible and UV irradiations.

Table 1. The reaction conditions of Mn/Cu/O/chitosan nanocomposites synthesized in this work.

| Sample no. | Precursor | T and t in hydrothermal method | T and t of calcination | Product |
|---|---|---|---|---|
| 1 | $Mn(NO_3)_2.4H_2O$ + onion | 180 ˚C , 12 h | – | Amorphous product |
| 2 | Sample 1 | – | 400 ˚C , 2 h | $Mn/Mn_2O_3$ nano/microstructures |
| 3 | Sample 2 + CuO + chitosan | – | – | Mn/Cu/O/chitosan nanocomposite |

T = Temperature , t = time

effective photocatalyst for MB degradation.

In continuation, the effects of the photocatalyst and dye concentrations for degradation of MB under visible light irradiation were investigated, as shown in Fig. 5. Fig. 5a shows the effect of the photocatalyst concentration on the degradation percentage of MB. In this research, three different weights of the photocatalyst were used, including 0.03, 0.05, and 0.07 g. This figure shows that the rate of photocatalytic degradation is proportional to the photocatalyst concentration. The Langmuir-Hinshelwood equation expresses a direct relationship between photocatalyst concentration and rate of dye degradation [19]. MB contaminant photodegradation in the presence of 0.07 g photocatalyst is 83 % after 75 min, as shown in Fig. 5a. Fig. 5b shows the evolution of the degradation of MB with irradiation time for three solutions with different concentrations, including 5, 10 and 15 ppm. This figure reveals with increasing dye concentration, the photocatalytic degradation is decreased. MB contaminant photodegradation with 5 ppm concentration is 89 % after 75 min, as shown in Fig. 5b. Thus in this work, optimum conditions for the synthesis of Mn/Cu/O/chitosan NCs with high photocatalytic activity are 5 ppm and 0.07 g concentrations of MB and photocatalyst, respectively.

## CONCLUSION

In conclusion, Mn/Cu/O/chitosan NCs were synthesized after two steps. First, $Mn/Mn_2O_3$ nano/microstructures were synthesized in the presence of onion via hydrothermal method. Then Mn/Cu/O/chitosan nanocomposites were synthesized using chitosan, CuO powder, and $Mn/Mn_2O_3$ prepared

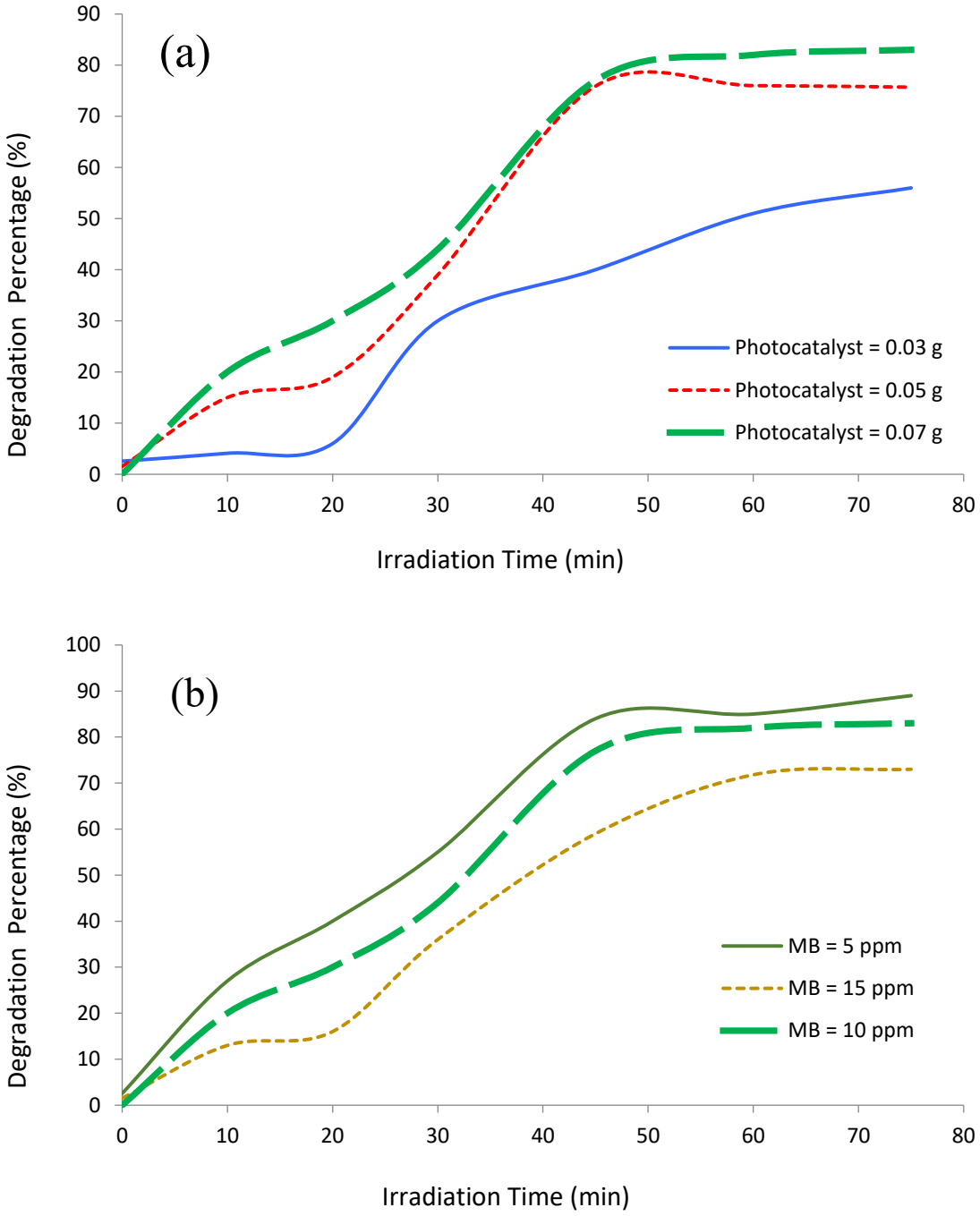


Fig. 5. Effects of: (a) photocatalyst and (b) dye concentrations for degradation of MB under visible light irradiation.

in the first step. The as-prepared nanocomposites were used as photocatalysts for MB degradation. The obvious degradation of MB was observed in the presence of these nanocomposites under visible irradiation. The photocatalytic performance of the nanocomposites was found influenced by the dye and photocatalyst concentrations. The optimum amount of photocatalyst was selected

0.07 g for the degradation of 5 ppm MB solution.

## ACKNOWLEDGEMENTS

Authors are grateful to the Kosar University of Bojnord for supporting this work.

## CONFLICT OF INTEREST

The authors declare that there is no conflict of interests regarding the publication of this manuscript.

## REFERENCES

1. Bayat S, Sobhani A, Salavati-Niasari M. $Co_2SiO_4$ nanostructures: New simple synthesis, characterization and investigation of optical property. Materials Research Bulletin. 2017;88:248-257.
2. Sobhani A, Salavati-Niasari M. Hydrothermal synthesis of CoSe nanostructures without using surfactant. J Mol Liq. 2016;220:334-338.
3. Sobhani A, Salavati-Niasari M. Cobalt selenide nanostructures: Hydrothermal synthesis, considering the magnetic property and effect of the different synthesis conditions. J Mol Liq. 2016;219:1089-1094.
4. Sobhani A, Salavati-Niasari M. Transition metal selenides and diselenides: Hydrothermal fabrication, investigation of morphology, particle size and and their applications in photocatalyst. Adv Colloid Interface Sci. 2021;287:102321.
5. Sobhani A, Salavati-Niasari M. CdSe nanoparticles: facile hydrothermal synthesis, characterization and optical properties. Journal of Materials Science: Materials in Electronics. 2015;26(9):6831-6836.
6. Aranaz I, Alcántara AR, Civera MC, Arias C, Elorza B, Heras Caballero A, et al. Chitosan: An Overview of Its Properties and Applications. Polymers. 2021;13(19):3256.
7. Wollner A, Lange F, Schmelz H, Knozinger H. Characterization of mixed copper-manganese oxides supported on titania catalysts for selective oxidation of ammonia. Applied Catalysis A: General. 1993;94(2):181-203.
8. Ahmad R, Kumar R. Adsorption studies of hazardous malachite green onto treated ginger waste. J Environ Manage. 2010;91(4):1032-1038.
9. Barka N, Qourzal S, Assabbane A, Nounah A, Ait-Ichou Y. Photocatalytic degradation of an azo reactive dye, Reactive Yellow 84, in water using an industrial titanium dioxide coated media. Arabian Journal of Chemistry. 2010;3(4):279-283.
10. Faouzi Elahmadi M, Bensalah N, Gadri A. Treatment of aqueous wastes contaminated with Congo Red dye by electrochemical oxidation and ozonation processes. J Hazard Mater. 2009;168(2-3):1163-1169.
11. Khadhraoui M, Trabelsi H, Ksibi M, Bouguerra S, Elleuch B. Discoloration and detoxicification of a Congo red dye solution by means of ozone treatment for a possible water reuse. J Hazard Mater. 2009;161(2-3):974-981.
12. Tehrani-Bagha AR, Nikkar H, Mahmoodi NM, Markazi M, Menger FM. The sorption of cationic dyes onto kaolin: Kinetic, isotherm and thermodynamic studies. Desalination. 2011;266(1-3):274-280.
13. Lal M, Mishra S. Characterization of Surface Runoff, Soil Erosion, Nutrient Loss and their Relationship for Agricultural Plots in India. Current World Environment. 2015;10(2):593-601.
14. Pathak S, Ranjan V, Tiwari S, Ranjan A, Tripathi A, Nagar A, et al. Case History: Largest Hydraulic Fracturing Jobs of India in KG Basin and Successful Production Test with Underbalanced Slim Hole Selective Completion in HPHT Environment. All Days; 2015/11/24: SPE; 2015.
15. International Research Journal of Engineering Science, Technology and Innovation.
16. Erratum: Sediment Benchmarks Based on Acid-Volatile Sulfide and Simultaneously Extracted Metals—When Is Organic Carbon Normalization Meaningful? Integr Environ Assess Manage. 2020;16(3):407-407.
17. Mohassel R, Sobhani A, Salavati-Niasari M, Goudarzi M. Pechini synthesis and characteristics of $Gd_2CoMnO_6$ nanostructures and its structural, optical and photocatalytic properties. Spectrochimica Acta Part A: Molecular and Biomolecular Spectroscopy. 2018;204:232-240.
18. Dong A, Wu H, Liu R, Wang Q, Fan X, Dong Z. Horseradish peroxidase-mediated functional hydrophobization of jute fabrics to enhance mechanical properties of jute/thermoplastic composites. Polymer Engineering & Science. 2020;61(3):731-741.
19. Sayılkan F, Asiltürk M, Tatar P, Kiraz N, Şener Ş, Arpaç E, et al. Photocatalytic performance of Sn-doped $TiO_2$ nanostructured thin films for photocatalytic degradation of malachite green dye under UV and VIS-lights. Materials Research Bulletin. 2008;43(1):127-134.